CHEMISTRY
A EUROPEAN JOURNAL

DOI: 10.1002/chem.200501613

# Kinetic Analysis of Semisynthetic Peroxidase Enzymes Containing a Covalent DNA–Heme Adduct as the Cofactor

**Ljiljana Fruk, Joachim Müller, and Christof M. Niemeyer*[a]**

**Abstract:** The reconstitution of apo enzymes with DNA oligonucleotide-modified heme (protoporphyrin IX) cofactors has been employed as a tool to produce artificial enzymes that can be specifically immobilized at the solid surfaces. To this end, covalent heme–DNA adducts were synthesized and subsequently used in the reconstitution of apo myoglobin (aMb) and apo horseradish peroxidase (aHRP). The reconstitution produced catalytically active enzymes that contained one or two DNA oligomers coupled to the enzyme in the close proximity to the active site. Kinetic studies of these DNA–enzyme conjugates, carried out with two substrates, ABTS and Amplex Red, showed a remarkable increase in peroxidase activity of the DNA–Mb enzymes while a decrease in enzymatic activity was observed for the DNA–HRP enzymes. All DNA–enzyme conjugates were capable of specific binding to a solid support containing complementary DNA oligomers as capture probes. Kinetic analysis of the enzymes immobilized by the DNA-directed immobilization method revealed that the enzymes remained active after hybridization to the capture oligomers. The programmable binding properties enabled by DNA hybridization make such semisynthetic enzyme conjugates useful for a broad range of applications, particularly in biocatalysis, electrochemical sensing, and as building blocks for biomaterials.

**Keywords:** DNA-directed immobilization · enzymes · kinetics · myoglobin · proteins

## Introduction

Protein microarrays are currently attracting increasing interest due to their potential as analytical tools for biomedical analysis and proteome research.[1–6] A general problem in the fabrication of protein biochips arises from the intrinsic instability of many proteins that often prohibits array preparation by stepwise, robotic immobilization of multiple proteins at chemically activated surfaces. To overcome these problems, we have developed the DNA-directed immobilization (DDI) of proteins as a chemically mild procedure for the highly parallel and reversible attachment of multiple proteins to a solid support by using a DNA microarray as the immobilization matrix.[7–9] To extend the DDI method to the fabrication of enzyme arrays, it is crucial to develop methodologies for synthesizing distinct DNA–enzyme conjugates that are well-defined with respect to their stoichiometric composition, that is, the number of DNA oligomers attached to the enzyme of interest, as well as the regioselectivity of coupling, that is, to control at which site of the enzyme the nucleic acid is coupled to.[10] Solutions to these problems can be achieved by using recombinant proteins containing reactive chemical sites, such as exposed cystein residues[11] or C-terminal thioesters,[12–14] which allow the selective tagging of the protein with the nucleic acid. We have recently demonstrated another feasible route to efficiently produce well-defined DNA–enzyme conjugates that involves the chemical modification of the heme cofactor with synthetic DNA oligonucleotides and the use of the DNA–heme adducts in the reconstitution of apo enzymes.[15] A similar approach was recently also applied to flavo-enzymes.[16]

Owing to the role of prosthetic groups in the catalytic activity of many enzymes, intensive research has been carried out within the last 50 years to investigate how structural alterations influence the properties of the respective enzymes. Examples include flavoenzymes,[17,18] pyrroloquinoline quinine,[19,20] and heme-containing[21,22] enzymes. Heme enzymes are particularly interesting as they catalyze a variety of redox reactions and are therefore powerful catalysts for synthetic organic chemistry.[23] Heme enzymes from different biological sources sometimes catalyze similar types of reaction

[a] Dr. L. Fruk, Dipl.-Chem. J. Müller, Prof. Dr. C. M. Niemeyer
Universität Dortmund, Fachbereich Chemie
Biologisch-Chemische Mikrostrukturtechnik
Otto-Hahn Strasse 6, 44227 Dortmund (Germany)
Fax: (+49) 231-755-7082
E-mail: christof.niemeyer@uni-dortmund.de

because of their structural similarity. For example, myoglobin (Mb) under certain conditions can act as peroxidases,[24–26] however, its peroxidase activity is much lower than that of classical peroxidases, such as horseradish peroxidase (HRP). Owing to its high stability and reactivity, HRP is the most widely used peroxidase,[27–29] and, with regard to synthetic chemistry, it can be employed as a catalyst for a broad range of reactions, such as oxidations of aromatic compounds, epoxidation, and enantioselective reduction of racemic hydroperoxides.[23,30]

Significant efforts have been undertaken to extend the versatility of heme enzymatic function and to enhance its catalytic activity by site-directed mutagenesis and/or cofactor modification. While the first approach is considered tedious and often impractical for certain enzymes, for example, cytochrome *c* peroxidase[31] or catalase,[32] the chemical modification of cofactors and its insertion into apo enzymes, that is, enzymes from which the natural cofactor has been removed, offers a variety of possibilities to change the enzymatic function by synthetic methods. For example, Hayashi and others were able to increase the peroxidase activity of myoglobin (Mb) by modifying the propionate side chains of the hemin with artificial functional groups.[33,34] Similarly, the oxygen affinity of the Mb was increased by replacing the native protoporphyrin IX with prophycene.[35] Watanabe and co-workers inserted chromium-containing salophen into several apo-Mb (aMb) mutants,[36] thereby producing artificial metalloenyzmes capable of catalyzing $H_2O_2$-dependent sulfoxidation of thioanisole. Ryabov and co-workers reconstituted HRP with ferrocene-modified hemin, thus leading to the increased activity of the enzyme towards organometallic substrates.[37] Chemically modified cofactors have also been utilized as anchors for the immobilization of enzymes at different surfaces. Extensive work in this area has been carried out by Willner and co-workers by using FAD derivatives to immobilize glucose oxidase at gold electrodes and to study the electrical contacting and electron transfer.[17,38,39]

Recently, we have shown that novel artificial Mbs can be generated by reconstitution of apo-Mb with covalent DNA–hemin conjugates.[15] The highly specific binding properties of the DNA moiety of the resulting Mb–DNA conjugate can be utilized for the specific DNA-directed immobilization (DDI) of the DNA–Mb conjugates both at the micrometer and nanometer length scales, thereby leading to applications in materials research[40] and the life sciences.[41,42] Interestingly, the reconstituted DNA–Mb conjugates showed enhanced peroxidase activity towards the substrate Amplex Ultra Red, even after they were immobilized at the solid surface by means of DDI. In that study, however, the catalytic properties of the DNA–Mb conjugates as well as the general applicability of the reconstitution to other heme enzymes have not been investigated in detail. Here we report on the continuation of this approach by further improving the synthesis of the covalent heme–DNA adducts and by applying the procedure to DNA oligomers of different length and base composition. Moreover, we extended our reconstitution approach to the enzyme horseradish peroxidase (HRP) and we carried out a thorough kinetic investigation of both Mb–DNA and HRP–DNA conjugates by using two different substrates, namely ABTS and Amplex Red (see below). This allowed us to quantify the activity of the enzyme–DNA conjugates both in the solution and immobilized at solid supports by means of the DDI method. The results provided initial insights into the catalytic cycles occurring during substrate transformation.

## Results and Discussion

**Synthesis of heme–DNA and reconstitution of apo enzymes**: Hemin (protoporphyrin IX) was activated in solution by using HBTU, HOBt, and DiPEA in DMF/$CH_3CN$ and coupled to amino-modified 12-mer oligonucleotide. Several different routes for DNA–heme adduct synthesis were investigated and, of those, amide coupling by using HBTU proved to be the most successful. The 12-mer oligonucleotide attached to the controlled porous glass (CPG) solid support was used for this reaction and coupling of activated hemin was performed after the trityl amino protecting group was removed by dichloroacetic acid treatment. The optimization of the coupling conditions (1 h, RT, 1 equiv HBTU, 0.75 equiv HOBt) led to the successful synthesis of two heme–DNA adducts. The HPLC trace (Figure 1) revealed that two products were formed in high yields and were identified by MALDI-TOF MS as the desired hemin–DNA adducts containing either one ($hemD_1$) or two DNA oligomers ($hemD_2$).

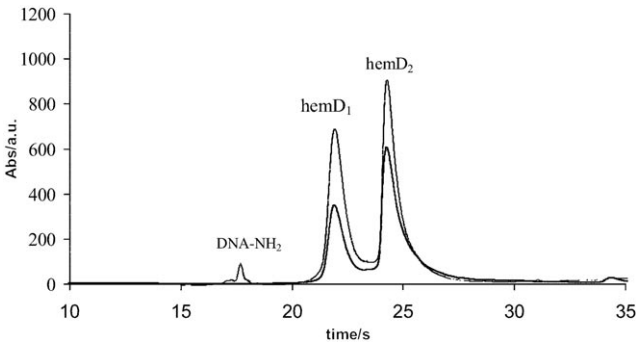


Figure 1. Reversed-phase HPLC purification of DNA–heme adducts. The solid line represents the absorbance at 405 nm and the dotted line the absorbance at 260 nm.

Apo-Mb and apo-HRP were prepared by the Teale butanone extraction method.[43] In brief, enzymes were dissolved in water (to make up a 50 μM solution) and acidified to either pH 2.5 (Mb) or pH 2.0 (HRP) with ice-cooled HCl (0.1 M). The extraction was performed with ice-cooled 2-butanone and the excess of solvent was removed by passing the solution through a Sephadex NAP-5 column. The concentration of the apo enzymes was determined spectrophotometrically. Freshly prepared apo enzymes were reconstituted with $hemD_1$ and $hemD_2$, leading to the DNA–enzyme

  

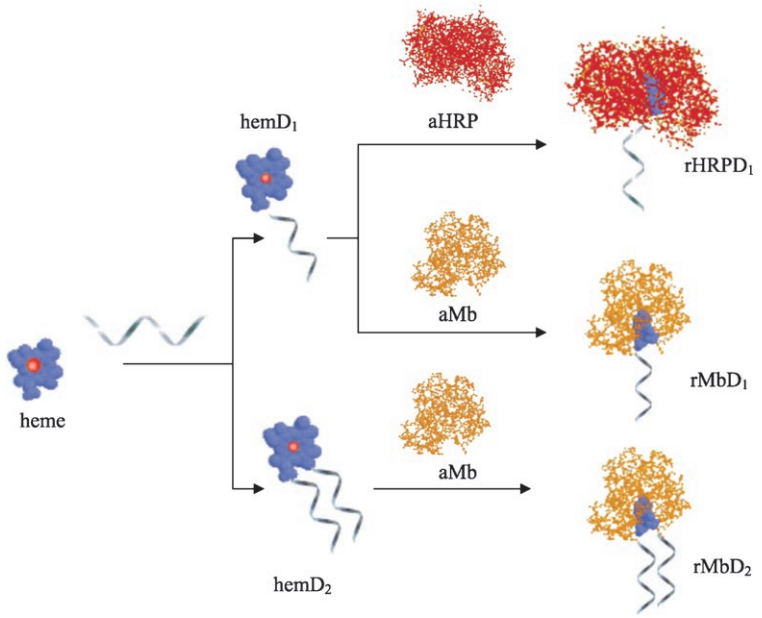


Figure 2. Reconstitution of apo-HRP and apo-Mb with DNA–heme conjugates. $HemD_1$ and $hemD_2$ are covalent DNA–heme adducts coupled with one or two DNA oligomers, respectively.

conjugates $MbD_1$, $MbD_2$, and $HRPD_1$, respectively (Figure 2). To synthesize non-DNA-modified enzymes as controls for enzyme kinetic studies, apo-Mb and apo-HRP were also reconstituted with commercially available hemin, leading to active enzymes, denoted as rMb and rHRP, respectively.

The semisynthetic enzyme–DNA conjugates were analyzed and purified by FPLC by using a linear gradient of 1.5 M NaCl in Tris buffer, pH 8.3, over 25 min. Representative chromatograms are shown in Figure 3. The significant differences in retention time of the apo- and DNA-reconstituted enzymes enabled the fast and efficient purification of the DNA–enzyme conjugates. In the case of Mb, reconstitution with both $hemD_1$ and $hemD_2$ adducts led to the DNA–Mb conjugates $MbD_1$ and $MbD_2$, respectively. Reconstitution of Mb with $hemD_1$ usually proceeded in almost quantitative yields, while $MbD_2$ and $HRPD_1$ yields varied between 80–90%. The time for completion of the reconstitution reaction varied for the two heme–DNA adducts such that 12 h were required for $hemD_1$ and 20 h for $hemD_2$ reconstitution.

In the case of apo-HRP, the reconstitution reaction exclusively led to the formation of the $HRPD_1$ that was completed after 12 h. Further attempts to reconstitute HRP with $hemD_2$ by varying the buffer conditions, such as pH and ionic strength, and varying temperatures, and increasing reaction times, remained unsuccessful. This observation suggested that the bulky heme with its two DNA oligomers is unable to enter the heme pocket, probably due to steric factors. This assumption is in agreement with protein crystal-structure data,[44] indicating that the heme pocket is buried deep inside the globular HRP. In contrast the heme pocket of Mb is located close to the surface of the protein[45] and, therefore, even the bulky $hemD_2$ adduct can enter the heme binding site of the protein.

UV/Vis spectrophotometric analysis of both $MbD_1$ and $MbD_2$ showed an absorbance maximum at 408 nm and of $HRPD_1$ at 403 nm (data not shown). These values are in agreement with literature data for the native enzymes.[46,47] In addition, we observed a broadened peak at 274 nm (Mb)

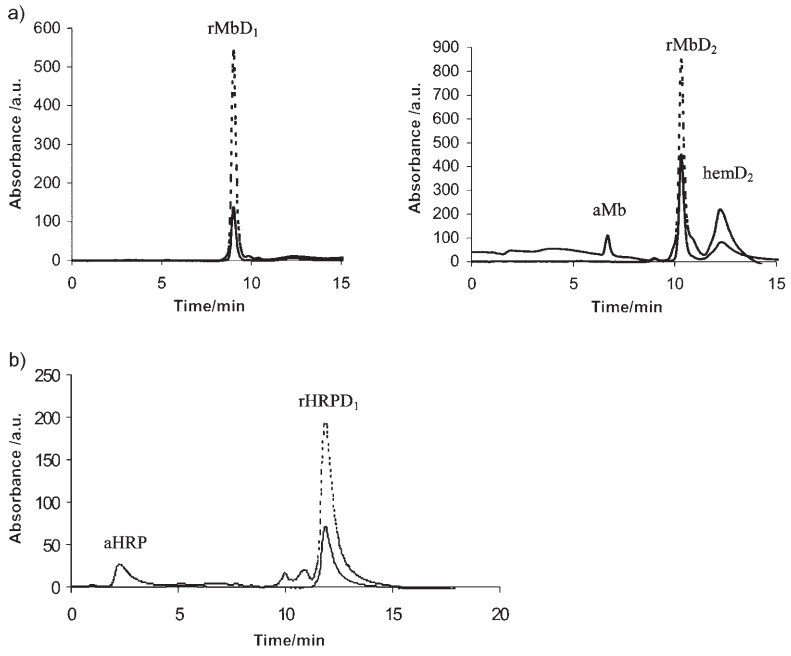


Figure 3. Fast protein liquid chromatograms of the reconstitution of: a) aMb with $hemD_1$ and $hemD_2$ and; b) aHRP with $hemD_1$. The dotted and solid lines indicate the absorbance measured at 280 and 405 nm, respectively.

and 279 nm (HRP) due to the absorbance of both the protein and the DNA moieties.

**Peroxidase activity of reconstituted enzymes**: Peroxidases catalyze the oxidation of a variety of substrates in the presence of hydrogen peroxides. In general, peroxidases initially react with $H_2O_2$ to generate the primary intermediate, called compound I. This intermediate undergoes two sequential one-electron reduction steps by the substrate to generate compound II and, again, the resting state of the enzyme. Both reductions lead to the formation of the final product. In view of the surprisingly high reactivity of both $MbD_1$ and $MbD_2$ observed in our initial description of these conjugates,[15] we were curious to study what particular effect on the catalytic activity of the pseudo peroxidase Mb and the real peroxidase HRP may arise from the linkage of DNA oligomers to the propionate side chains of the prosthetic heme group. To this end, we chose two typical substrates, Amplex Red and ABTS, which are often used in peroxidase reactions.

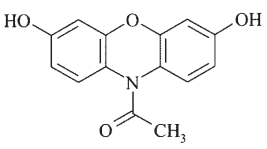


Amplex Red

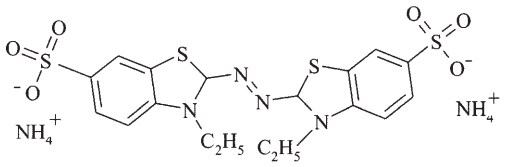


ABTS

Amplex Red is frequently employed in a range of enzymatic assays because of its sensitivity and stability. In the presence of peroxidases, the nonfluorescent Amplex Red substrate reacts with $H_2O_2$ in a 1:1 molar ratio to produce the brightly fluorescent product resorufin.[48] The substrate ABTS reacts with peroxidases to produce a radical cation that strongly absorbs at 405 nm, thereby allowing the detection of low levels of peroxidases.[49]

To demonstrate that the DNA stays chemically stable during the oxidative conditions of the enzymatic assays, we incubated the 12-mer oligonucleotide in a typical assay solution containing ABTS (0.2 mM) and $H_2O_2$ (2.0 mM) for 30 min at room temperature. Subsequent HPLC analysis revealed no detectable changes in the elution profile, thus indicating that the DNA was not affected by the conditions of the enzyme assay.

To obtain the kinetic parameters for the peroxidase activity we used the simplified model of a multisubstrate reaction by varying the substrate concentration while keeping constant an excess concentration of $H_2O_2$. Since the kinetic parameters in multisubstrate reactions are functions of both substrate and $H_2O_2$ concentration, the ultimate values obtained by this method were considered to be apparent constants.

The reactions were monitored by using a microplate reader for the collection of absorbance (ABTS) or fluorescence (Amplex Red) data. The data were analyzed by using the Michaelis–Menten theory by applying Equation (1), in which [S] represents the concentration of the substrate, that is, ABTS or Amplex Red, $[E]_0$ is the total amount of the enzyme used, and the $v_0$ is the initial rate of reaction determined experimentally. Hyperbolic curves were obtained after plotting $v_0/[E]_0$ against the substrate concentration. A nonlinear curve fitting was carried out to obtain the Michaelis–Menten parameters. Figure 4 shows typical curves obtained from native and reconstituted HRP. The numeric data of the Michaelis–Menten parameters and the catalytic efficiency, usually expressed as the $k_{cat}/K_M$ ratio, obtained for HRP-transformation of both substrates are shown in Table 1.

$$\frac{v_0}{[E]_0} = \frac{k_{cat}[S]}{K_M + [S]} \quad (1)$$

As indicated by the catalytic efficiency ($k_{cat}/K_M$) data, native HRP showed a notably higher activity with both substrates than the reconstituted enzymes, rHRP and rMb, respectively. A slight decrease in activity was observed when the cofactor was removed and subsequently replaced into the native enzyme (that is, rHRP), while a significant decrease was observed for the DNA-containing $HRPD_1$ conjugate. Removal and insertion of heme can lead to the destruction of the hydrogen-bonding network which, together with incomplete protein re-folding upon reconstitution, may account for the decrease of the rHRP activity observed. However, the strong increase in the $K_M$ value and the only 50% decrease in the $k_{cat}$ value of $HRPD_1$ suggested that this effect is not the only reason for the observed change in catalytic efficiency. It was previously shown that substrates, in particular aromatic molecules, bind to HRP close to the *δ-meso* edge of the heme ring.[50] Owing to the fact that the bulky DNA oligomer is attached close to the *δ-meso* edge of the heme, the DNA is likely to sterically hinder the binding of the ABTS substrate and, therefore, contribute to the lower affinity and the decreased activity observed.

The comparison of the $K_M$ data in Table 1 also indicates that the affinity for the polar ABTS (1897 μM for $HRPD_1$ compared to 233 μM for nHRP) is affected to a larger extent than that for the nonpolar Amplex Red (125 μM for $HRPD_1$ compared to 106 μM for nHRP), whereas the $k_{cat}$ values of $HRPD_1$ are reduced to about one third of those of the native HRP, regardless of the polarity of the substrate. These observations strongly suggest additional electrostatic repulsion between the negatively charged DNA strand and the ABTS substrate. As an additional reason for the changes in catalytic performance, one may also speculate about indirect effects occurring from interactions between the DNA

  

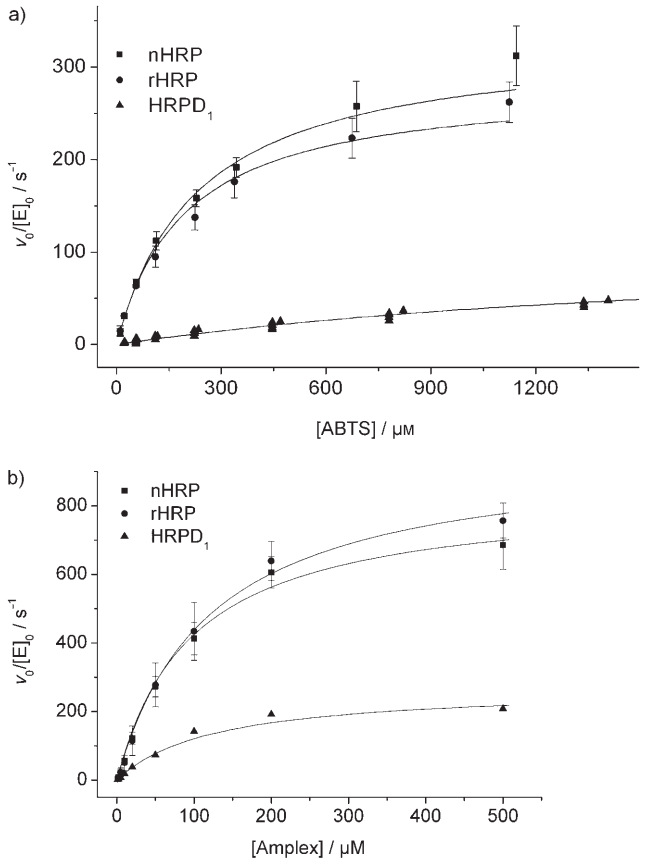


Figure 4. Data and curve-fitting performed to obtain Michaelis–Menten parameters for ABTS (a) and Amplex Red (b) transformation by native HRP (nHRP) and reconstituted HRP (rHRP and $HRPD_1$). The enzyme concentrations were 1 nM (a) and 0.1 nM (b).

In view of the immobilization experiments described below, we also measured the catalytic activity of $HRPD_1$ in the presence of two molar equivalents of complementary DNA strands (cD in Table 1, entry 4). The decrease in catalytic activity to about 50% of the value observed for the single-stranded species was observed. This observation correlates well with the hypothesis described above of increased steric hindrance and electrostatic repulsion resulting from the formation of bulky negatively-charged dsDNA in close proximity to the active site of the HRP.

Interestingly, the DNA conjugation also had a marked effect on the long-term stability of HRP at low concentrations. While the activity of a 100 nM nHRP solution decreased significantly with storage time (to about 75% after eight days), $HRPD_1$ showed an almost unchanged activity even after two months of storage (data not shown). Similar to that previously observed for other DNA–protein conjugates,[11] this increase in stability might result from the increased polarity of the DNA–enzyme conjugate reducing intermolecular aggregation and nonspecific adsorption of the conjugate to the walls of the storage vessel that otherwise induce partial denaturation of the enzyme and, thus, gives a loss in catalytic activity.

We further studied the enzyme kinetics of Mb conjugates which, in general, showed a dramatically different catalytic efficiency pattern to that of HRP. As mentioned above, the main physiological function of the Mb concerns the reversible storage of oxygen in muscle, and it can also function as a pseudo peroxidase in the presence of $H_2O_2$. As such, Mb follows the typical peroxidase catalytic cycle in the presence of $H_2O_2$ and forms the $MbFe^{IV}{=}O$ species that corresponds to compound I of peroxidases.[52] Here, $MbD_1$ and $MbD_2$ showed a significant increase in activity with both substrates, and in particular, with Amplex Red. However, the distinct reactivity patterns of the various Mb conjugates were quite different for the two substrates under investigation. Figure 5 shows typical curves obtained from the transformation of ABTS by native and reconstituted Mb enzymes. The numeric data of the Michaelis–Menten parameters are summarized in Table 2.

Table 1. Kinetic parameters of the catalytic oxidation of ABTS and Amplex Red by $H_2O_2$ in the presence of nHRP, rHRP, and $HRPD_1$.

| | | ABTS | | | Amplex Red | | |
|---|---|---|---|---|---|---|---|
| Entry | Enzyme | $k_{cat}$ [$s^{-1}$] | $K_M$ [μM] | $k_{cat}/K_M$ [$\mu M^{-1}\,s^{-1}$] | $k_{cat}$ [$s^{-1}$] | $K_M$ [μM] | $k_{cat}/K_M$ [$\mu M^{-1}\,s^{-1}$] |
| 1 | nHRP | 332±18 | 233±21 | 1.42±0.15 | 860±38 | 106±13 | 8±1 |
| 2 | rHRP | 284±16 | 195±15 | 1.11±0.07 | 969±44 | 123±14 | 7.9±1.0 |
| 3 | $HRPD_1$ | 107±8 | 1897±238 | 0.057±0.008 | 271±5 | 125±14 | 2.2±0.3 |
| 4[a] | $HRPD_1$+cD | n.d. | n.d. | n.d. | 155±4 | 138±9 | 1.12±0.08 |

[a] Owing to the higher sensitivity of detection, Amplex Red substrate was used both for the study of DNA hybridization and the immobilization experiments (see Table 4).

moiety and the outer surface of the protein. It is known that the propionate chains of the heme influence the heme orientation as well as the reactivity of compound I by the formation of an extensive hydrogen-bonding network with surrounding amino acid residues of the HRP, and the esterification of the propionate groups has been shown to induce perturbances in the entry and binding of anionic substrates that caused destabilization of compound I.[51] It is, therefore, possible that the DNA strand engages in the hydrogen-bonding network thereby lowering the affinity for the substrate, thus leading to an increase in the $K_M$ value.

The determination of the Michaelis–Menten parameters revealed that the catalytic efficiency ($k_{cat}/K_M$) for $MbD_2$ (Table 2, entry 3) is more than fourfold higher than that of nMb (Table 2, entry 1). This result contradicts the expectation that the accumulation of negative charges at the DNA sugar–phosphate backbone should hinder the entrance of the negatively charged ABTS to the heme pocket. Instead, the $K_M$ values determined indicated that $MbD_2$ has a significantly higher substrate affinity than nMb. An explanation might be deduced from the tertiary structure of horse heart Mb, previously determined by X-ray crystallographic analy-

  

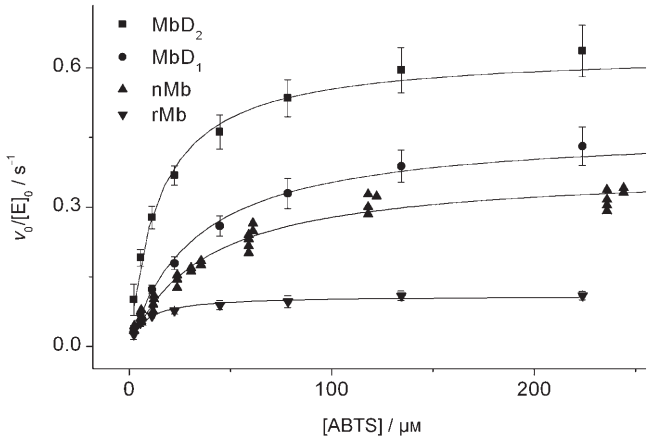


Figure 5. Data and curve-fitting performed to obtain Michaelis–Menten parameters for ABTS oxidation with native and reconstituted Mb enzymes. The enzyme concentration was 100 nM.

Table 2. Kinetic parameters of the catalytic oxidation of ABTS by native and reconstituted Mb enzymes.

| Entry | Enzyme | $k_{cat}$ [$s^{-1}$] | $K_M$ [μM] | $k_{cat}/K_M$ [$\mu M^{-1} s^{-1}$] |
|---|---|---|---|---|
| 1 | nMb | $0.41 \pm 0.02$ | $44 \pm 4$ | $0.0094 \pm 0.001$ |
| 2 | $MbD_1$ | $0.47 \pm 0.005$ | $33 \pm 1.7$ | $0.0144 \pm 0.0011$ |
| 3 | $MbD_2$ | $0.63 \pm 0.02$ | $14.4 \pm 1.5$ | $0.044 \pm 0.004$ |

sis.[45] Mb has several basic residues near the heme pocket, and it was previously observed that additional carboxylic acid groups of non-natural heme analogues are effectively neutralized by these basic residues.[33] Therefore, it is plausible that they also neutralize the negative charges of the phosphate backbone of the DNA, thereby minimizing the electrostatic repulsion between the substrate and the DNA-containing substrate-binding site.

Monzani and co-workers have demonstrated that the introduction of hydrogen donor and acceptor groups to the heme influences the hydrogen-bond network of the Mb, thereby leading to a slight rigidification of the active site and an increased stability of compound I.[53] This study also showed that the heme-binding pocket is not sufficiently large to entirely accommodate peptide-modified heme derivatives and the peptide-carrying propionate chains rather extend to the outside of the heme pocket. Therefore, we hypothesize that the increased reactivity of the $MbD_2$, observed here, may result from steric constraints of the DNA strands leading to an opening of the active site, thereby facilitating an increased accessibility for substrate molecules. This hypothesis could also explain the increase in $k_{cat}$ values observed. All these effects of the DNA attachment on the Mb reactivity were similarly observed for the $MbD_1$ conjugate, however, they were apparent to a smaller extent.

Kinetic studies of the oxidation of Amplex Red by the various Mb enzymes revealed that, similar to ABTS, the catalytic efficiency of $MbD_2$ is higher than that of $MbD_1$ and both DNA enzymes are far more active than the native Mb. Moreover, a very distinctive biphasic behavior was observed in the Amplex Red reaction, indicating that a slow reaction rate occurs at low and a significantly faster rate at high substrate concentrations (Figure 6a and b, respectively). Biphasic behavior of Mb catalysis was previously observed by Monzani and co-workers, and it was explained by two consecutive binding interactions between the enzyme and the substrate.[53] As shown in Scheme 1, both consecutive substrate binding interactions lead to the generation of product. The first reaction pathway ($K_{D1}$, $k_1$) is dominant at low sub-

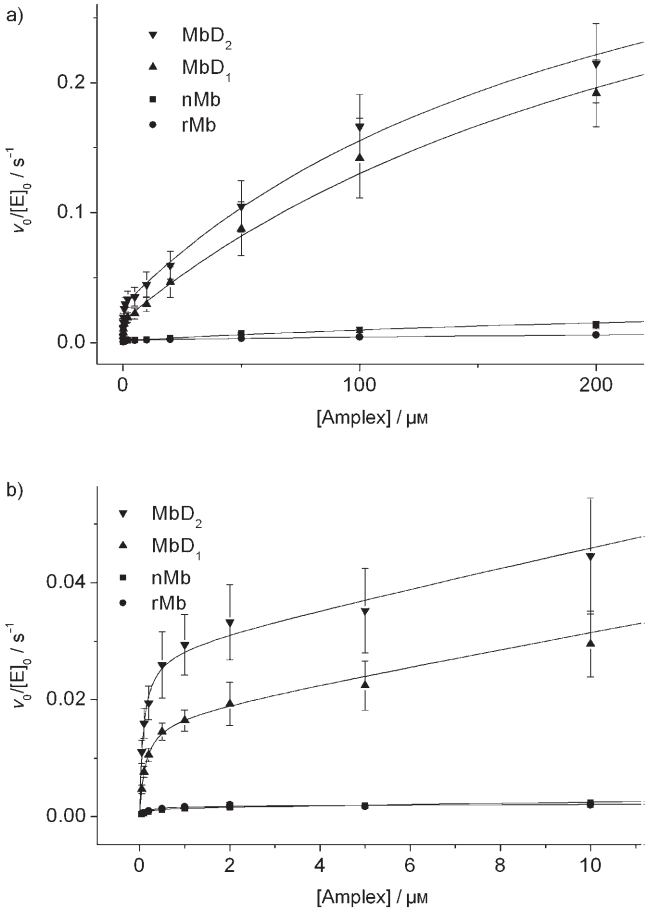


Figure 6. Data and curve-fitting performed to obtain Michaelis–Menten parameters for the biphasic Amplex Red oxidation with native and reconstituted Mb enzymes. Curves in (a) show the entire concentration range measured while the curves in (b) are enlarged to show the reaction rates at low substrate concentration. The enzyme concentrations were 10 nM.

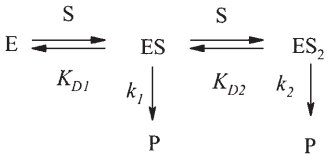


Scheme 1. Consecutive reaction pathways of Mb, according to reference [53].

  

strate concentration. It is saturated quickly leading to an intermediary plateau thereby allowing the second reaction pathway ($K_{D2}$, $k_2$) to occur at higher substrate concentrations.

The data obtained were fitted by weighted nonlinear regression by using Equation (2) derived for biphasic behavior by Monzani and co-workers, where $k_1$ and $k_2$ are the rate constants for the oxidation of the protein-bound substrate in mono (ES) and bis ($ES_2$) adducts, respectively. $K_{D1}$ and $K_{D2}$ are the two dissociation constants associated with the interactions. By using this model, the kinetic parameters were calculated and the results are shown in Table 3.

$$\frac{\nu_0}{[E]_0} = \frac{\frac{k_1[S]}{K_{D1}} + \frac{k_2[S]^2}{K_{D1}K_{D2}}}{1 + \frac{[S]}{K_{D1}} + \frac{[S]^2}{K_{D1}K_{D2}}} \quad (2)$$

Table 3. Kinetic parameters of the biphasic catalytic oxidation of Amplex Red by native and reconstituted Mb enzymes.

| Entry | Enzyme | $k_1$ [$10^{-3}$ s$^{-1}$] | $K_{D1}$ [μM] | $k_1/K_{D1}$ [$10^{-3}$μM$^{-1}$ s$^{-1}$] | $k_2$ [$10^{-3}$ s$^{-1}$] | $K_{D2}$ [μM] | $k_2/K_{D2}$ [$10^{-3}$μM$^{-1}$ s$^{-1}$] |
|---|---|---|---|---|---|---|---|
| 1 | nMb | 1.48±0.05 | 0.14±0.02 | 11±2 | 43±21 | 407±223 | 0.11±0.08 |
| 2 | rMb | 1.82±0.07 | 0.15±0.02 | 11.9±1.4 | 16±6 | 499±293 | 0.03±0.02 |
| 3 | $MbD_1$ | 17.0±0.5 | 0.128±0.009 | 133±11 | 450±59 | 283±64 | 1.6±0.4 |
| 4 | $MbD_1$+cD | 4.8±0.4 | 0.014±0.009 | 334±199 | 386±72 | 403±84 | 1.0±0.3 |
| 5 | $MbD_2$ | 28.5±1.2 | 0.082±0.009 | 348±43 | 432±63 | 218±51 | 2.0±0.5 |
| 6 | $MbD_2$+cD | 14.1±0.4 | 0.008±0.004 | 1735±950 | 325±96 | 387±139 | 0.8±0.4 |

Similar to that observed for the ABTS substrate, the values in Table 3 indicate that both rate constants $k_1$ and $k_2$ are increased for the DNA–Mb conjugates as compared to the nMb. $K_{D1}$ and $k_1$, which were obtained from the low substrate concentration curve of the biphasic model, suggest that the DNA enzymes have a high affinity for the substrate at low concentrations. We used the ratio of the second set of parameters, $k_2$ and $K_{D2}$, derived from the higher substrate concentration range, as a measure of the catalytic efficiency. The comparison of $k_2/K_{D2}$ data revealed a remarkable increase in enzymatic activity, namely $MbD_2$ (Table 3, entry 5) and $MbD_1$ (Table 3, entry 3) were 18 and 15 times more active than the nMb (Table 3, entry 1). The reasons for this increase in catalytic efficiency should be similar to those discussed above for the transformation of ABTS.

**Kinetic study of immobilized enzymes**: According to our concept, the DNA moieties are intended to be used as programmable handles for DNA-directed self-assembly and immobilization. Therefore, kinetic measurements were also carried out in the presence of DNA oligomers that are complementary to the heme-bound DNA (cD, 5′biotin-GGT GAA GAG ATC-3′, entries 4 and 6 in Table 3). To investigate the effects of the hybridization with cD on the enzymatic performance, Amplex Red was chosen as a substrate because of the higher sensitivity as compared to the ABTS reaction. Initial measurements were carried out in solution with both $HRPD_1$ (Table 1, entry 4) as well as with $MbD_1$ and $MbD_2$ (Table 3, entries 4 and 6, respectively). The catalytical efficiency of $HRPD_1$+cD was reduced to about 50% (1.12 versus 2.2 μM$^{-1}$ s$^{-1}$ for $HRPD_1$) upon hybridization with complementary DNA. This result is in agreement with the general trend observed for the HRP–DNA conjugate, that is, the reduction of catalytic activity due to the presence of DNA closely attached to the active site of the enzyme. Although the activity of both dsDNA–Mb conjugates was still almost tenfold higher than that of nMb, a similar reduction in Mb–DNA activity was observed upon hybridization with complementary DNA oligomers. In the case of $MbD_1$+cD the $k_2/K_{D2}$ values were reduced to 62.5% (1.0 versus $1.6\times10^{-3}$ μM$^{-1}$ s$^{-1}$) and with $MbD_2$+cD to about 44% (0.8 versus $2.0\times10^{-3}$ μM$^{-1}$ s$^{-1}$) of the activity of the respective single-stranded Mb–DNA conjugates. These observations correlate with the hypothesis discussed above that steric hindrance and electrostatic repulsion of the bulky dsDNA reduces the access of the substrate to the reaction site.

We then measured the catalytic performance of the DNA–enzyme conjugates bound to the surface of microtiter plates by means of DDI. To this end, streptavidin-coated microplates were functionalized with biotinylated capture oligomers complementary to the heme-bound DNA and the DNA–enzyme conjugates were allowed to bind to the DNA-functionalized wells of the microplate (Figure 7).

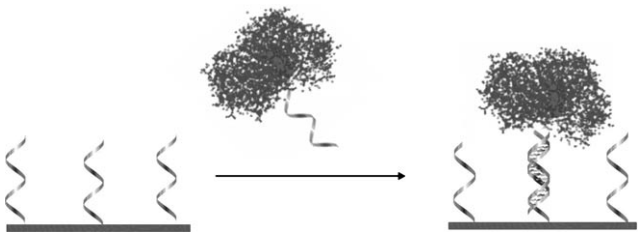

Figure 7. DNA-directed immobilization of cofactor-modified peroxidases.

Control assays were also carried out in wells that contained non-complementary capture oligomers. In these controls, no enzymatic activity was detected, indicating that the immobilization, indeed, occurred exclusively by specific Watson–Crick base pairing between the enzyme-bound DNA and the capture sequence. Kinetic measurements with immobilized enzymes were then carried out under similar conditions as reported for the measurements in solution. Typical plots of the $\nu_0/[E]_0$ values against the substrate concentration are shown in Figure 8. The kinetic study revealed that for both enzymes the substrate inhibition occurred at the high substrate concentration range. This threshold for inhibition was less than 50 μM for $MbD_1$ and $MbD_2$ and ap-

  

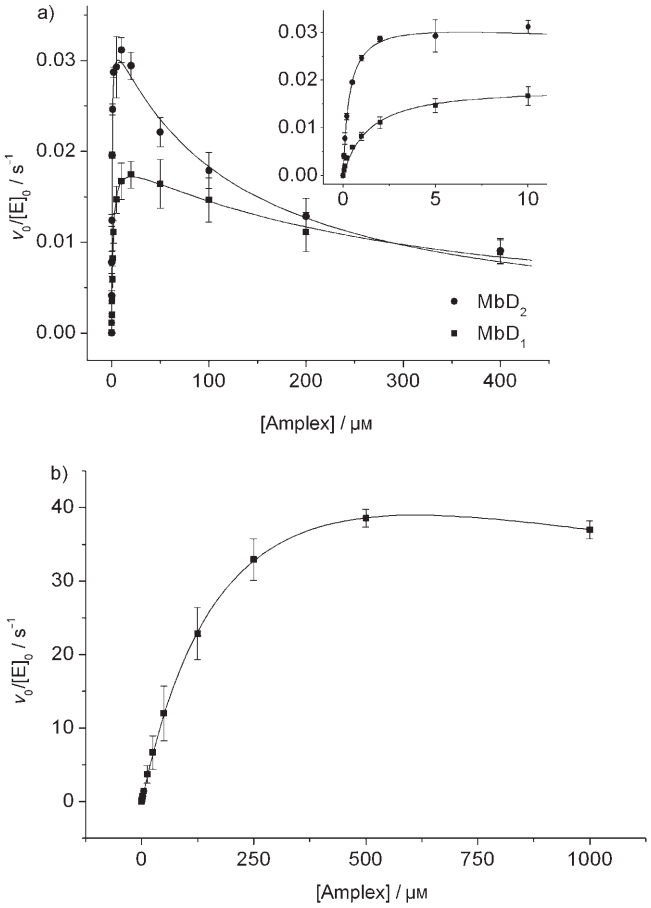


Figure 8. Data and curve-fitting obtained from Amplex Red oxidation with immobilized DNA–enzyme conjugates: a) Mb; b) HRP. The inset in a) shows the low concentration range for the Mb reaction.

The catalytic efficiency of immobilized HRP was approximately sevenfold lower than the activity measured in the solution. In the case of Mb, direct comparison is more difficult because the immobilized Mb–DNA conjugates did not reveal the biphasic behavior that had been observed in the experiments in solution. This suggested that the second binding proposed in Scheme 1 did not occur when the enzyme is immobilized at the solid support. Instead, an inhibition was observed similar to that of the HRP–DNA conjugates, and the fitting model provided a set of kinetic parameters (Table 4), which are no longer comparable directly to the biphasic model data of the in-solution reaction. However, the qualitative comparison of the data obtained from the low substrate concentration range in solution and those of the immobilized enzymes, depicted in Figure 9, suggested

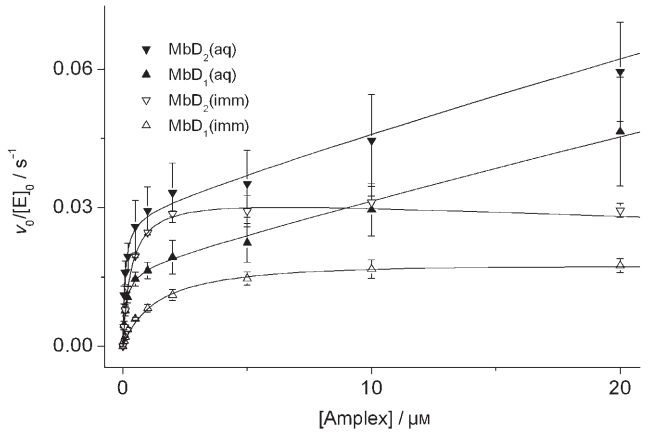


Figure 9. Comparison of the data and curve-fits for in-solution and immobilized $MbD_1$ and $MbD_2$ at low Amplex Red concentrations.

proximately 1000 μM for $HRPD_1$. It seems likely, that the inhibition occurred due to a restricted diffusion of substrates at the solid–liquid interphase because the immobilization leads to an orientation of the heme pocket of the enzyme towards the surface (Figure 7).

To obtain Michaelis–Menten parameters we therefore used Equation (3), which takes into account the effects occurring from substrate inhibition.[54] The numeric data are summarized in Table 4.

$$\frac{v_0}{[E]_0} = \frac{k_{cat}[S]}{K_M + [S]\left(1 + \frac{[S]}{K_S}\right)} \quad (3)$$

Table 4. Kinetic parameters of immobilized DNA–enzyme conjugates for the oxidation of Amplex Red.

| Entry | Enzyme | $k_{cat}$ [$s^{-1}$] | $K_M$ [μM] | $k_{cat}/K_M$ [$s^{-1}\mu M^{-1}$] | $K_s$ [μM] |
|---|---|---|---|---|---|
| 1 | $HRPD_1$ | 69 ± 1 | 242 ± 7 | 0.30 ± 8 | 1552 ± 82 |
| 2 | $MbD_1$ | 0.0196 ± 0.0004 | 1.4 ± 0.1 | 0.014 ± 0.012 | 300 ± 22 |
| 3 | $MbD_2$ | 0.0332 ± 0.0006 | 0.34 ± 0.04 | 0.098 ± 0.011 | 124 ± 9 |

that the catalytic efficiencies are within the same order of magnitude. Moreover, the saturation step for the immobilized enzymes occurred at concentrations of less than 5 μM. This is similar to the plateau observed during the in-solution measurements. Hence, the immobilization apparently prevents the enzyme from following the second reaction pathway, characterized by $K_{D2}$ and $k_2$ in Scheme 1, and rather favors an inhibitive pathway that is restricted by orientation-derived factors, as discussed for the HRP immobilization. Nonetheless, although the catalytic activity of myoglobin decreased upon the immobilization, both $MbD_2$ and $MbD_1$ conjugates still revealed a much higher activity than the native Mb. This suggested that the effects responsible for the increase in enzymatic activity in solution persist even when the enzyme is bound to solid supports.

## Conclusion

We reported here on the successful generation of artificial peroxidase enzymes, myoglobin (Mb), and horseradish peroxidase (HRP) by reconstitution of the respective apo en-

  

zymes with covalent DNA–heme cofactor adducts. The kinetic studies of the peroxidase activity of those enzyme conjugates revealed that the catalytic activity of the reconstituted HRP species was decreased as compared to the native HRP. In contrast, the activity of the pseudo peroxidase Mb was significantly increased, as compared to the native Mb, upon the reconstitution with heme–DNA adducts, and Mb modified with two DNA strands was even more active than Mb containing a single DNA moiety. Detailed kinetic analyses of the apparent Miachelis–Menten parameters of the DNA–HRP and DNA–Mb conjugates provided supporting evidence for several factors, such as steric hindrance and electrostatic repulsion of the substrate by the bulky DNA strand closely attached to the active site. However, to fully unravel the molecular mechanisms responsible for the distinct changes in catalytic performances observed, the elucidation of the tertiary structure of the conjugate will be necessary, for instance, by molecular modeling and/or crystallographic analysis.

All the reconstituted DNA–enzyme conjugates were capable of binding to the solid surface through specific DNA-directed immobilization, and kinetic analysis with the Amplex Red substrate showed that an inhibition occurred at high substrate concentrations that was not observed in the measurements in solution. The highly specific binding properties of the DNA moiety offer excellent promise for the assembly of the heme enzymes both on micrometer and nanometer length scales. Considering the vast number of important heme enzymes, we believe that this method holds great potential in producing functional heme protein arrays or building blocks for nanostructured devices as well as in the development of transducer elements for novel biosensors.

## Experimental Section

**Chemicals**: Myoglobin (horse heart) and horseradish peroxidase were purchased from Sigma. *N*-acetyl-3,7-dihydroxyphenoxazin (Amplex Red), Quant-IT protein kit was obtained from Molecular Probes, and detritylation agent (3% DCA in DCM) from Amersham Biosciences. $H_2O_2$ was obtained from Fluka and a fresh solution prepared before the experiments. All other chemicals including hemin, *o*-(benzotriazol-1-yl)-*N*,*N*,*N*′,*N*′-tetramethyluronium hexafluorophosphate (HBTU), hydroxybenzotriazole (HOBt), and 2,2′-azino-bis-(3-ethylbenzthiazolin-6-sulfonate (ABTS) were obtained from Sigma–Aldrich and were used without further purification.

**Synthesis of $hemD_1$ and $hemD_2$**: Amino-modified oligonucleotide (5′Tramino-GAT CTC TTC ACC) that was still coupled to the CPG support and that contained the protection groups, was purchased from Tib Molbiol, Berlin, Germany. The trityl group was manually removed by using commercial 3% DCA in DMF solution followed by washing with $CH_3CN$ and drying with nitrogen. Hemin (75 μmol) and HBTU (75 μmol) were dissolved in 1.5 mL DMF and to this HOBt (50 μmol) in 500 μL DMF:$CH_3CN$ was added followed by 27 μL DiPEA. This solution was mixed with the detritylated oligonucleotide and coupling was allowed to proceed for 60 min at room temperature. The hemin-modified oligonucleotide was then deprotected by using *tert*-butylamine:MeOH:HO (1:2:1) mixture for 3 h at 65 °C and purified by HPLC, similar as previously described.[15]

**Reconstitution**: Apo-Mb (aMb) and apo-HRP (aHRP) were prepared by the Teale 2-butanone method.[43] In brief, a solution of the apo enzyme (200 μL, 60 μM) in potassium phosphate buffer, pH 7, was mixed with hemin, $hemD_1$, or $hemD_2$ (1.1 equiv, 330 μL,40 μM), and was incubated for 2, 12, or 24 h, respectively, at 4 °C. Reconstituted enzymes were purified by using ion-exchange FPLC (AKTA purifier, Amersham Bioscience, MonoQ column, buffer A: 20 mM Tris A pH 8.3 and buffer B: 20 mM Tris A and 1.5 M NaCl, linear gradient over 25 min). The concentration was determined spectrophotometrically and additionally confirmed by using a Quant-IT protein quantification kit.

**Enzyme kinetics**: Kinetic experiments were carried out by using a Synergy HT microplate reader from BioTek (running Software KC4, Version 3.4, Revision 12) in transparent (ABTS) and black (Amplex Red) 96-well microplates. In all experiments 50 μL enzyme solution or 50 μL buffer (used as a blank) was added to the microplate wells. The solutions were kept at a constant temperature of 25 °C for 5 min. At the same time the substrate/$H_2O_2$ solution was prepared and kept at a constant temperature of 25 °C and the reaction was started by adding 50 μL to the wells containing enzyme or blank. The reaction progress was monitored for 20 min as described below. The time interval between two measurements was 30 s. KC4 Software (BioTek) was used for the analysis of primary data. The initial rate of each experiment was derived by linear regression analysis of the linear range of the time versus background-corrected absorbance or fluorescence values. Further calculations and weighted nonlinear regressions were performed by using MS Excel and Origin software packages.

ABTS solution in 50 mM phosphate/citrate buffer, pH 5.0, containing 300 mM NaCl was freshly prepared every day before measurements, and the actual ABTS concentration was determined by using the molar extinction coefficient of $\varepsilon_{340} = 36000\ cm^{-1}\ mol^{-1}$. Enzymatic reactions were monitored by using the absorbance of the ABTS cation radical produced (molar extinction coefficient $\varepsilon_{405} = 36800\ cm^{-1}\ mol^{-1}$). The final concentrations of myoglobin enzymes and horseradish peroxidases were 100 and 1 nM, respectively. All reaction solutions contained 2 mM $H_2O_2$.

Amplex Red stock solutions were prepared according to the manufacturer's instructions by using potassium phosphate buffer with 300 mM NaCl, pH 7.4. Variable concentrations of Amplex Red were used while the concentration of $H_2O_2$ was fixed at 1 mM. The rate of the reactions was followed by monitoring the fluorescence of the reaction product resorufin at 590 nm, by using the excitation wavelength of 530 nm. The final concentration of myoglobin enzymes was 10 nM and that of horseradish peroxidases 0.1 nM.

**DNA-directed immobilization (DDI)**: DDI of the DNA–enzyme conjugates $MbD_1$, $MbD_2$, and $HRPD_1$ was carried out by using streptavidin-coated microplates that had been previously functionalized with biotinylated capture oligomers (5′biotin-GGT GAA GAG ATC), similar as previously described.[55] Controls were carried out in wells functionalized with non-complementary oligomers (5′biotin-CAG GAT GGT CTT). Saturation experiments indicated that the maximum loading of enzyme per well is approximately 0.5 pmol (data not shown). Subsequent to DDI-based enzyme immobilization, 100 μL of Amplex Red solutions of different concentrations was added to each well and the fluorescence emission monitored at 590 nm ($\lambda_{ex}$ 530 nm).

## Acknowledgements

This work was supported by the European Union (project STREP 013775) and Marie Curie Incoming International Fellowship (project 514582) to L.F. and the Zentrum für Angewandte Chemische Genomik, a joint research initiative founded by the European Union and the Ministry of Innovation and Research of the state North Rhine Westfalia. We would like to thank Prof. Roger Goody for helpful discussions on peroxidase kinetics.

[1] H. Zhu, M. Snyder, *Curr. Opin. Chem. Biol.* **2001**, *5*, 40–45.
[2] R. L. Stears, T. Martinsky, M. Schena, *Nat. Med.* **2003**, *9*, 140–145.

  

[3] K. B. Lee, J. H. Lim, C. A. Mirkin, *J. Am. Chem. Soc.* **2003**, *125*, 5588–5589.
[4] M. B. Soellner, K. A. Dickson, B. L. Nilsson, R. T. Raines, *J. Am. Chem. Soc.* **2003**, *125*, 11790–11791.
[5] J. A. Camarero, Y. Kwon, M. A. Coleman, *J. Am. Chem. Soc.* **2004**, *126*, 14730–14731.
[6] K. Zhang, M. R. Diehl, D. A. Tirrell, *J. Am. Chem. Soc.* **2005**, *127*, 10136–10137.
[7] C. M. Niemeyer, T. Sano, C. L. Smith, C. R. Cantor, *Nucleic Acids Res.* **1994**, *22*, 5530–5539.
[8] R. Wacker, C. M. Niemeyer, *ChemBioChem* **2004**, *5*, 453–459.
[9] R. Wacker, H. Schroeder, C. M. Niemeyer, *Anal. Biochem.* **2004**, *330*, 281–287.
[10] C. M. Niemeyer in *Nanobiotechnology: Concepts, Methods and Applications* (Eds.: C. M. Niemeyer, C. A. Mirkin), Wiley-VCH, Weinheim, **2004**, pp. 227–243.
[11] F. Kukolka, C. M. Niemeyer, *Org. Biomol. Chem.* **2004**, *2*, 2203–2206.
[12] M. Lovrinovic, R. Seidel, R. Wacker, H. Schroeder, O. Seitz, M. Engelhard, R. Goody, C. M. Niemeyer, *Chem. Commun.* **2003**, 822–823.
[13] M. Lovrinovic, M. Spengler, C. Deutsch, C. M. Niemeyer, *Mol. BioSyst.* **2005**, *1*, 64–69.
[14] M. Lovrinovic, C. M. Niemeyer, *Biochem. Biophys. Res. Commun.* **2005**, *333*, 943–948.
[15] L. Fruk, C. M. Niemeyer, *Angew. Chem.* **2005**, *117*, 2659–2662; *Angew. Chem. Int. Ed.* **2005**, *44*, 2603–2606.
[16] P. Simon, C. Dueymes, M. Fontecave, J.-L. Decout, *Angew. Chem.* **2005**, *117*, 2824–2827; *Angew. Chem. Int. Ed.* **2005**, *44*, 2764–2767.
[17] Y. Xiao, F. Patolsky, E. Katz, J. F. Hainfeld, I. Willner, *Science* **2003**, *299*, 1877–1881.
[18] G. Tedeschi, A. Negri, F. Ceciliani, A. Mattevi, S. Ronchi, *Eur. J. Biochem.* **1999**, *260*, 896–903.
[19] O. A. Raitman, F. Patolsky, E. Katz, I. Willner, *Chem. Commun.* **2002**, 1936–1937.
[20] A. R. Dewanti, J. A. Duine, *Biochemistry* **1998**, *37*, 6810–6818.
[21] G. C. Wagner, M. Perez, W. A. Toscano, Jr., I. C. Gunsalus, *J. Biol. Chem.* **1981**, *256*, 6262–6265.
[22] E. J. Tomlinson, S. J. Ferguson, *Proc. Natl. Acad. Sci. USA* **2000**, *97*, 5156–5160.
[23] H. Waldmann, K. Drauz, *Enzyme Catalysis in Organic Synthesis*, Wiley-VCH, Weinheim, **2002**.
[24] D. Keilin, E. F. Hartree, *Biochem. J.* **1955**, *60*, 310–325.
[25] P. George, D. H. Irvine, *Biochem. J.* **1952**, *52*, 511–517.
[26] B. Kalyanaraman, R. P. Mason, B. Tainer, T. E. Eling, *J. Biol. Chem.* **1982**, *257*, 4764–4768.
[27] K. G. Welinder, L. B. Smillie, G. R. Schonbaum, *Can. J. Biochem.* **1972**, *50*, 44–62.
[28] K. G. Welinder, L. B. Smillie, *Can. J. Biochem.* **1972**, *50*, 63–90.
[29] W. Zhang, G. Li, *Anal. Sci.* **2004**, *20*, 603–609.
[30] W. Adam, Z. Lukacs, C. R. Saha-Moller, P. Schreier, *Biochim. Biophys. Acta* **1999**, *1427*, 236–244.
[31] M. Wilming, A. Iffland, P. Tafelmeyer, C. Arrivoli, C. Saudan, K. Johnsson, *ChemBioChem* **2002**, *3*, 1097–1104.
[32] C. Jakopitsch, G. Regelsberger, P. G. Furtmuller, F. Ruker, G. A. Peschek, C. Obinger, *J. Inorg. Biochem.* **2002**, *91*, 78–86.
[33] T. Hayashi, Y. Hisaeda, *Acc. Chem. Res.* **2002**, *35*, 35–43.
[34] I. Hamachi, T. Nagase, Y. Tajiri, S. Shinkai, *Bioconjugate Chem.* **1997**, *8*, 862–868.
[35] T. Hayashi, H. Dejima, T. Matsuo, H. Sato, D. Murata, Y. Hisaeda, *J. Am. Chem. Soc.* **2002**, *124*, 11226–11227.
[36] M. Ohashi, T. Koshiyama, T. Ueno, M. Yanase, H. Fujii, Y. Watanabe, *Angew. Chem.* **2003**, *115*, 1035–1038; *Angew. Chem. Int. Ed.* **2003**, *42*, 1005–1008.
[37] A. D. Ryabov, V. N. Goral, L. Gorton, E. Csöregi, *Chem. Eur. J.* **1999**, *5*, 961–967.
[38] A. Riklin, E. Katz, I. Willner, A. Stocker, A. F. Buckmann, *Nature* **1995**, *376*, 672–675.
[39] M. Zayats, E. Katz, I. Willner, *J. Am. Chem. Soc.* **2002**, *124*, 2120–2121.
[40] C. M. Niemeyer, W. Bürger, J. Peplies, *Angew. Chem.* **1998**, *110*, 2391–2395; *Angew. Chem. Int. Ed.* **1998**, *37*, 2265–2268.
[41] C. M. Niemeyer, J. Koehler, C. Wuerdemann, *ChemBioChem* **2002**, *3*, 242–245.
[42] C. M. Niemeyer, *Trends Biotechnol.* **2002**, *20*, 395–401.
[43] F. W. Teale, *Biochim. Biophys. Acta* **1959**, *35*, 543.
[44] G. I. Berglund, G. H. Carlsson, A. T. Smith, H. Szoke, A. Henriksen, J. Hajdu, *Nature* **2002**, *417*, 463–468.
[45] S. V. Evans, G. D. Brayer, *J. Mol. Biol.* **1990**, *213*, 885–897.
[46] V. Sanz, S. de Marcos, J. R. Castillo, J. Galban, *J. Am. Chem. Soc.* **2005**, *127*, 1038–1048.
[47] D. Puett, *J. Biol. Chem.* **1973**, *248*, 4623–4634.
[48] M. Zhou, Z. Diwu, N. Panchuk-Voloshina, R. P. Haugland, *Anal. Biochem.* **1997**, *253*, 162–168.
[49] R. E. Childs, W. G. Bardsley, *Biochem. J.* **1975**, *145*, 93–103.
[50] R. Z. Harris, S. L. Newmyer, P. R. Ortiz de Montellano, *J. Biol. Chem.* **1993**, *268*, 1637–1645.
[51] S. Adak, R. K. Banerjee, *Biochem. J.* **1998**, *334*, 51–56.
[52] N. K. King, M. E. Winfield, *J. Biol. Chem.* **1963**, *238*, 1520–1528.
[53] E. Monzani, G. Alzuet, L. Casella, C. Redaelli, C. Bassani, A. M. Sanangelantoni, M. Gullotti, L. de Gioia, L. Santagostini, F. Chillemi, *Biochemistry* **2000**, *39*, 9571–9582.
[54] R. A. Capeland, *Enzymes- A Practical Introduction to Structure, Mechanism and Data Analysis*, Wiley, New York, **2000**.
[55] C. M. Niemeyer, W. Bürger, R. M. J. Hoedemakers, *Bioconjugate Chem.* **1998**, *9*, 168–175.

Received: December 22, 2005
Revised: February 21, 2006
Published online: July 10, 2006

  